ROYAL SOCIETY OF CHEMISTRY

PAPER

CrossMark
click for updates

Formation of nanoscopic CaF$_2$ *via* a fluorolytic sol–gel process for antireflective coatings†

Alexander Rehmer, Kerstin Scheurell and Erhard Kemnitz*

The synthesis of nanoscopic calcium fluoride was performed by the fluorolytic sol–gel process. Antireflective coatings of CaF$_2$ were prepared from sols obtained by the reaction of CaCl$_2$ with HF and subsequent dip coating. The addition of tetramethyl orthosilicate (TMOS) or tetraethyl orthosilicate (TEOS) after fluorination promotes the formation of transparent sols. The formation and crystallisation of CaF$_2$ nanoparticles was studied by ^{19}F liquid and solid state NMR spectroscopy, dynamic light scattering (DLS) and X-ray powder diffraction (XRD). The morphology of a CaF$_2$-film was analysed by high resolution scanning electron microscopy (HR-SEM) and the mechanical stability of a CaF$_2$-film was evaluated by the Crockmeter test using both felt and steel wool. The refractive index for a CaF$_2$-film was measured by ellipsometry. The synthesis of CaF$_2$ nanoparticles derived from CaCl$_2$ is a good way to achieve porous antireflective coating layers.

Introduction

Calcium fluoride and other metal fluorides exhibit superior optical properties. Their optical transmittance ranges from low UV up to the high IR region. For example, calcium fluoride is a dielectric material with an optical window ranging from 0.13 to 10 μm (ref. 1) exhibiting a broad spectrum of optical applications like IR, UV, microscope, astronomical instrumentation and spectroscopy. Especially the use of calcium fluoride as ceramic material for laser applications is advantageous because not only the mechanical and optical properties compared with single crystals of calcium fluoride are better but it can be produced in large volumes.[2–4] Furthermore, calcium fluoride and magnesium fluoride own a low refractive index (CaF$_2$: n = 1.44 at 500 nm MgF$_2$: n = 1.38 at 500 nm).[1,5] Thus, calcium fluoride and magnesium fluoride are promising candidates for antireflective (AR) coatings. If the refractive index of the coating is lower than the refractive index of the substrate, the reflection of the light will decrease. The complete anti-reflection for single coatings depends on the mean geometric refractive index of the AR-layer with $n_1{}^2 = n_s n_0$ and its thickness with $n_1 d = \lambda/4$, where n_1, n_S and n_0 are the refractive indices of the coating, substrate and air, respectively, d the thickness of the film and λ the wavelength of the light.[6] For example, common glass mainly built up by SiO$_2$ (n_S = 1.55 at 500 nm) usually is surrounded by the medium air (n_0 = 1.0). Hence, the optimum refractive index is n_1 = 1.22. For destructive interference, the antireflective coating is one quarter of the wavelength of light. In this case, the thickness of the AR-layer should be 102 nm. Thus, CaF$_2$ is a good candidate to decrease the reflection of the incident light of glass. A comparison between CaF$_2$ and MgF$_2$ shows similar optical properties. Only the solubility in water reveals that CaF$_2$ (16 mg L^{-1}) is less soluble than MgF$_2$ (76 mg L^{-1}).[7] This is a factor, which could be interesting for the chemical resistance of an AR-layer against outdoor conditions like rain or moisture. Due to its very low solubility, CaF$_2$-films could be more weatherproof than MgF$_2$-films.

It is well known, that porous antireflective alkaline earth metal fluoride films can be prepared by spin coating from sols of calcium trifluoroacetate.[8] That is, calcium trifluoroacetate sols in water/isopropanol are first prepared by reacting trifluoroacetic acid and calcium acetate. From the sols obtained this way a surface layer of calcium trifluorocacetate can be created by spin coating. The following annealing initiates the thermal decomposition of the trifluoroacetate resulting in a porous calcium fluoride layer as reported in *J. Sol-Gel Sci. Technol.*[9] The disadvantage of this method is the thermal decomposition of the metal trifluoroacetates into toxic and corrosive reaction products like CF$_3$COF, COF$_2$ and HF. Another point is that a mixture of metal acetate and trifluoroacetic acid may yield metal oxide fluoride phases leading to an increase of the refractive index due to the oxygen content inside the film.

In this paper, we present an easy synthesis approach toward nanoscaled CaF$_2$-sols *via* the fluorolytic sol–gel process to fabricate finally antireflective CaF$_2$-films by dip-coating. For excellent AR-layers, it is necessary to start from a transparent sol with particle sizes of about 10 to 20 nm or smaller. The choice of the solvent is an important factor because only volatile solvents

Humboldt-Universität zu Berlin, Department of Chemistry, Brook-Taylor-Str. 2, 12489 Berlin, Germany. E-mail: erhard.kemnitz@chemie.hu-berlin.de; Fax: +49 30 2093 7277

like *e.g.* methanol, ethanol, and isopropanol lead to homogeneous layers.

Here, we report a way to use the cost-efficient synthesis of calcium fluoride sols with commercially available calcium chloride precursors by reaction with anhydrous HF. The influence of TMOS to the calcium fluoride sol is investigated as well as the optical and mechanical properties of the calcium fluoride films obtained from thus prepared CaF_2-sols.

Experimental

Precursor synthesis

All chemicals for the synthesis of calcium fluoride are commercially available and need no drying or further processing. The 19.84 M HF-solution was prepared by dissolving anhydrous HF in ethanol.

A series of under-stoichiometric calcium fluoride sols with fluorine to calcium ratios F : Ca < 2 was prepared by dissolution of 1.33 g anhydrous $CaCl_2$ (96% ABCR, 12 mmol) in ethanol (99.8%, ROTH, 0.4 M solution). Under vigorous stirring at ambient conditions, the required amount of HF-solution was added dropwise to the solution.

The stoichiometric calcium fluoride sol (Ca : F = 1 : 2) for coating on glass slides (Borosilicate) was prepared by the reaction of 8.88 g of $CaCl_2$ (80 mmol) with 8 mL of HF (160 mmol; 2 eq.) in 192 mL ethanol. After fluorination 0.59 mL of TMOS (5 mol% of Ca) respectively 0.88 mL of TEOS (5 mol% of Ca) was added. The influence of TMOS was studied by ^{19}F NMR.

Deposition of CaF_2 coating films

A typical procedure for the deposition of calcium fluoride coating films was as follows. The freshly prepared calcium fluoride sols were deposited on borosilicate glass by dip-coating. Before the coating experiment the glass slides were cleaned in an alkaline solution (RBS®50) for 15 min. The substrates were rinsed with deionized water and dried by blowing compressed air. After the coating, the substrates were calcined in a vented air-oven (Barnstead Thermolyne type F48000) at 500 °C for 15 min followed by slow cooling down to room temperature.

Materials characterization

The calcium fluoride sols were characterized by dynamic light scattering (DLS) and ^{19}F liquid NMR spectroscopy. The DLS measurements were performed using a Zetasizer Nano ZS (Malvern instruments, Worcestershire, UK) using disposable PMMA cuvettes. Hydrodynamic diameters were calculated from the correlation functions by the Malvern Nanosizer Software. The viscosity was determined simultaneously to DLS measurements with a microviscometer from Anton Paar (AMVn, Graz, Austria) at 25 °C. The ^{19}F NMR spectra of the sols with varying fluorine content were carried out using a Bruker AVANCE II 300 (liquid state NMR spectrometer with a Larmor frequency of 282.4 MHz). The ^{19}F isotropic chemical shifts are given with respect to the $CFCl_3$ standard.

The Transmission Electron Microscope (TEM) analysis has been carried out using a Philips CM200 LaB_6 microscope operating at 200 kV. A few drops of the solution containing the nanoparticles have been deposited on a carbon-coated copper grid and let them dry prior to the inspection.

The calcium fluoride xerogels were characterized by an X-ray powder diffractometer from Seifert (XRD 3003 TT) and by ^{19}F solid state NMR spectroscopy. The static ^{19}F solid state NMR spectra were recorded with a Bruker AVANCE 400 (solid state spectrometer, Larmor frequency of 376.4 MHz) with a 4 mm Bruker probe and the ^{19}F MAS NMR spectra were recorded with a 2.5 mm Bruker probe. The ^{19}F isotropic chemical shifts are given with respect to C_6F_6 as secondary standard with $\delta_{iso} = -166.6$ ppm against $CFCl_3$. Rotor-synchronized Hahn spin-echo experiments (rs-echo) were performed which react sensitive on homonuclear dipolar couplings. This means that fluorine species with an effective spin exchange (short spin-spin relaxation times T_2, *i.e.* well-bridged species) are not or with decreased intensity detected after applying longer dipolar evolution times, whereas those with longer spin–spin relaxation times (not well-incorporated, terminal) are detected. The number of rotor periods before echo detection (L0) is given in the figure captions. The percentage of chloride in the xerogels was determined by elemental analysis.

The surfaces of calcium fluoride films were examined by high-resolution scanning electron microscopy (HR-SEM) from Zeiss (Supra 40). The refractive index $n_{(500\ nm)}$ and thickness t of the CaF_2-layers was determined by spectroscopic ellipsometry. The ellipsometric parameters psi and delta were measured with a SENpro instrument (Sentech, Berlin, Germany) with the software "SpectraRay3". The calculated parameters psi and delta are determined with a Sellmeier model. The reflection and absorption of the CaF_2-film was measured with an UV-Vis-spectrometer (Shimadzu UV-3100, Kyoto, Japan), in the range of 300–1400 nm.

The mechanic stability of the CaF_2-films was tested by a crockmeter from Erichsen (scratchmarker 249) using felt and steel wool with a fineness of 0000. The stamp with a contact area of 4.5 cm^2 was pressed on the sample with a force of 4 N.

Results and discussion

The fluorolytic sol–gel synthesis consists of the reaction between a suitable metal precursor and anhydrous hydrogen fluoride in a suitable organic solvent, preferentially methanol or ethanol.[10] Several calcium precursors like $Ca(OMe)_2$, $Ca(OEt)_2$, $Ca(OAc)_2$ and $CaCl_2$ were investigated. In most of the cases, metal alkoxides like $Si(OMe)_4$, $Ti(O^iPr)_4$ and $Al(O^iPr)_3$ or $Mg(OMe)_2$, respectively, are used in the classical oxide sol–gel route.[11–14] In case of the fluorolytic sol–gel synthesis, the synthesis of transparent CaF_2 sols starting from calcium alkoxides is not recommended because of the insolubility of the calcium alkoxide in methanol and ethanol at room temperature. Thus, $Ca(OMe)_2$ and $Ca(OEt)_2$ always form crystalline white precipitates of their $Ca(OR)_2 \cdot 4\ ROH$ solvates. By subsequent de-solvation fine crystalline powders with a three-dimensional polymeric structure of the CdI_2 type are formed.[15]

Unfortunately, it is impossible to obtain transparent CaF_2-sols under these circumstances; however, starting from calcium acetate suspended in an ethanol/acetic acid solution results in the formation of transparent CaF_2-sols but the stability of these sols is poor. That means, after a few days the CaF_2-sol is completely transformed to a gel. The reason for strong gelation tendency is esterification of acetic acid with the corresponding alcohol and the release of water. The more water is formed in the system the faster gelation occurs (eqn (1)).

$$AcOH + ROH \rightleftarrows AcOR + H_2O \qquad (1)$$

In spite of the gelation, coatings from these sols are possible for a short time only. The optical properties of such coatings are good but the mechanical properties are very poor due the high porosity in the film.[16] Thus, calcium acetate as precursor for calcium fluoride coatings is not recommended. Therefore, we decided to use calcium chloride as precursor instead because of its good solubility in alcohol and the absence of an esterification reaction. Following the general synthesis approach of MgF_2-sols *via* the fluorolytic sol–gel route by reacting $MgCl_2$ in EtOH with anhydrous HF,[17] we started from $CaCl_2$ in EtOH and reacted it with ethanolic HF solution to form nanoscopic calcium fluoride sols (eqn (2)).

$$CaCl_2 + 2HF_{EtOH} \rightarrow nano\ CaF_2 + 2HCL \qquad (2)$$
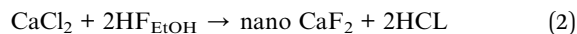
The transparency of the CaF_2-sol is opaque. By addition of 5 mol% tetramethyl orthosilicate (TMOS) or tetraethyl orthosilicate (TEOS) after fluorination the former opaque sol turned into a transparent CaF_2-sol. The reaction of $CaCl_2$ in ethanol with two equivalents of ethanolic HF solution leads to the formation of nanoscopic CaF_2 particles. For good optical and mechanical properties of an AR-layer the sol should be transparent to achieve a homogenous layer on the substrate. Beside sol-transparency as an indication for homodispersed nano-particle distribution, volatility of the solvent is a further pre-condition to obtain homogeneous coatings. The higher the volatility of the solvent is, the faster a homogenous film is formed. Although methanol is more volatile than ethanol, it is toxic compared to ethanol. Hence, the latter was used in all experiments. The formation of calcium fluoride nanoparticles was investigated by ^{19}F NMR spectroscopy. The amount of HF to calcium chloride was varied from 0.1 : 1 to 2 : 1 in order to follow species that might be formed in the course of reaction. The ^{19}F NMR spectra of the sols with different amount of HF are listed in Fig. 1. For a better illustration of the spectra without the known background signal in the ^{19}F liquid NMR, the samples were measured statically by solid state NMR. The liquid ^{19}F NMR spectra are included in the ESI.† Fig. 1 shows the typical signal for calcium fluoride at −108 ppm. Additionally to the CaF_2 signal a second broad signal appears at about −95 ppm and −93 ppm in the ^{19}F liquid NMR, respectively. We speculated, it may stand for another calcium fluoride species like calcium chloride fluoride (CaClF) or calcium alkoxide fluoride ($CaF_{2-x}OR_x$), which could be a solvated species. For further information of this species ^{19}F solid state NMR and XRD measurements of the xerogels were
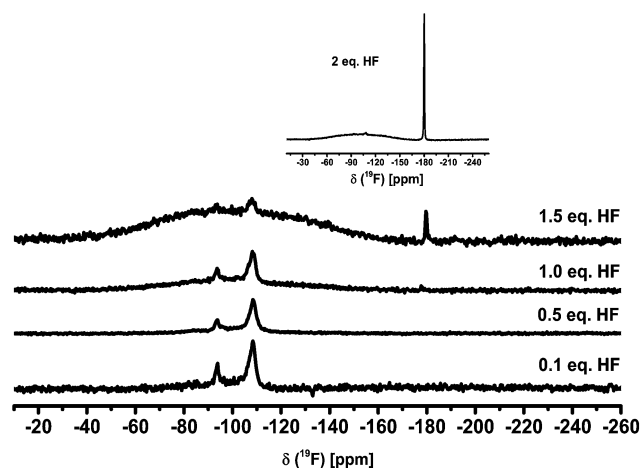

Fig. 1 ^{19}F NMR spectra of the sols with different fluorine content (normalized to the CaF_2 signal) carried out with ss-NMR spectrometer.

performed. Furthermore, the reaction of $CaCl_2$ with two equivalents of HF exhibits a broad signal in the static solid state ^{19}F NMR as well as in the liquid ^{19}F NMR at about −180 ppm (line width ~2000 Hz). Samples with under-stoichiometric amounts of fluorine also contain a signal between −174 ppm and −180 ppm in the liquid NMR. This signal corresponds to unreacted HF adsorbed to the particle surface.[18,19] A similar observation was made in the synthesis of MgF_2 *via* the fluorolytic sol–gel route, with either $Mg(OMe)_2$ or $MgCl_2$ as reaction. Thus, we speculate that this corresponds to HF adsorbed at the precursor.[17] During ageing of the MgF_2-sol the signal vanishes.

The addition of TMOS or TEOS to the CaF_2-sol vanishes this signal completely in a short time. The formation of $SiOR_{4-x}F_x$ and SiF_6^{2-} species (the second broad signal around −128 ppm could be $CaSiF_6$ (Fig. 2)) after TMOS/TEOS addition are further evidences for unreacted HF in the sols at this stage of nanoparticles surface causes agglomeration, but consequently, removal of this leads to clear sols. Due to the line width of ~4000 Hz the sol consists not only of calcium fluoride particles but also of calcium hexafluorosilicate or other fluorosilicate
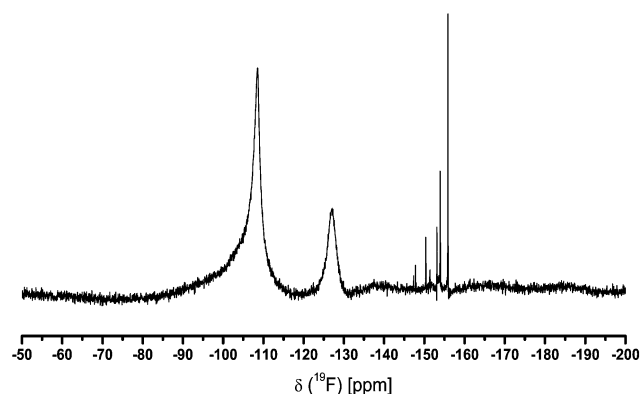

Fig. 2 ^{19}F NMR spectrum of a CaF_2-sol with 5 mol% of TMOS. Two broad signals at −108 ppm (CaF_2) and −128 ppm (SiF_6^{2-}, SiF_x) are observed. No evidence for adsorbed HF (liquid NMR spectrometer).

particles. The other small signals with line width of about 100 Hz are probably dissolved $SiOR_{4-x}F_x$ species. Both species evidently are formed from unreacted HF and added $Si(OMe)_4$. All as-prepared CaF_2-sols with 5 mol% TMOS or TEOS are transparent and possess low viscosity. Without addition of TMOS or TEOS the sol remains turbid and tends to form a gel. After a few days the particles are aggregated, that a settle to the bottom of the flask is observed, which is referred to as sedimentation of the sol. According to Fig. 3 the mean particle diameter of a sol with 5 mol% TMOS was determined by dynamic light scattering. The intensity weighted particle distribution shows two size classes with mean particle diameters of 20 nm and 320 nm. Due to the Stokes–Einstein relation bigger particles scatter much more than smaller particles because the intensity of scattering is proportional to the sixth magnitude of its diameter (Rayleigh approximation). It follows that small particles are significantly under-estimated. Hence, calculating the volume weighted particle distribution from intensity weighted one shows that in fact just one class of particles with a mean particle diameter of approximately 10 nm is present. In addition, the particle size was also investigated by transmission electron microscopy and results are included in the ESI.† For the identification of species with the characteristic ^{19}F NMR signal between −93 to −95 ppm ^{19}F solid state NMR measurements were performed. For an exact identification of the unknown species, the CaF_2-sol without the addition of TMOS was dried at room temperature in air and calcined at 600 °C in an electric furnace. The samples were compared with crystalline CaClF, which was synthesized by solid state reaction between $CaCl_2$ and CaF_2 in presence of NH_4Cl as flux at 730 °C for 3 h in an electric furnace. Wenz et al. reported an eutectic point at 645 °C for a composition of 18.5 mol% $CaCl_2$ and 81.5 mol% CaF_2.[20] Fig. 4 shows the ^{19}F MAS signal of the crystalline CaClF compound with a chemical shift of −83 ppm. The difference between the CaClF shift and the shift of the unknown species is about 12 ppm. Hence, the unknown species does not correspond to CaClF. The most plausible explanation is that this signal corresponds to an oxide fluoride species, which
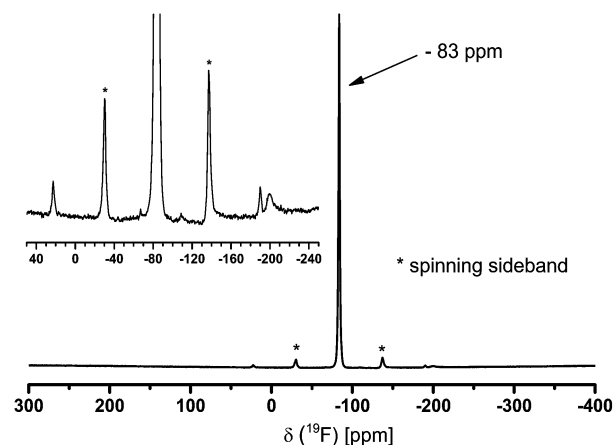

Fig. 4 ^{19}F MAS NMR spectrum (ν_{rot} = 20 kHz) of crystalline CaClF (rorisite) prepared from 40 mol% $CaCl_2$ and 60 mol% CaF_2 with NH_4Cl as flux at 730 °C for 3 h.

probably is caused by a preferential oxygen donation in the second coordination sphere as was also found for the MgF_2 system.[18] For comparison, the annealed CaF_2 xerogel with one equivalent of HF shows a decrease of the signal at −95 ppm and an increase of the signal at −83 ppm in the spectrum unlike the un-annealed sample (Fig. 5). Thus, the formation of CaClF in the sol for the system $CaCl_2$ in EtOH can be ruled out, it will only be formed at high temperature. Furthermore, the ^{19}F signal at about −95 ppm also appears in the NMR spectra of CaF_2-xerogels that have been prepared from other calcium precursors like $CaBr_2 \cdot H_2O$ and CaO which do not contain any chloride. The NMR spectra are listed in the ESI (Fig. S1–S3†). In the ^{19}F ss-NMR spectrum of the CaF_2-xerogel obtained from CaO with two equivalents of HF appears the corresponding signal as shoulder of the main signal of CaF_2. The difference between the signal shapes in the CaO–HF system and the $CaCl_2$/$CaBr_2$–HF system might be caused by dipole–dipole coupling. The shorter the dipole–dipole coupling is, the more is the signal separated from the main signal. Another interesting fact is also the different
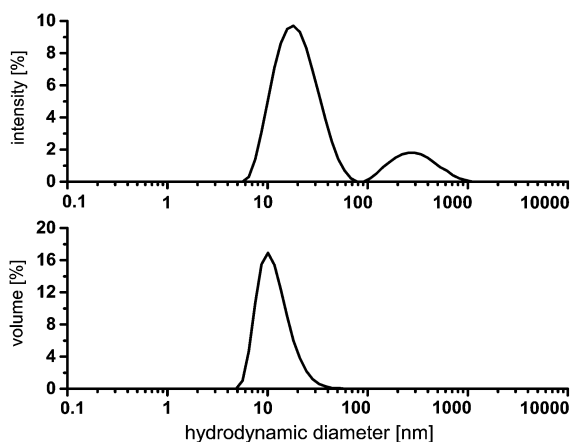

Fig. 3 Hydrodynamic diameter of particles of CaF_2-sol with 5 mol% TMOS measured by dynamic light scattering (intensity and volume weighted particle distribution).
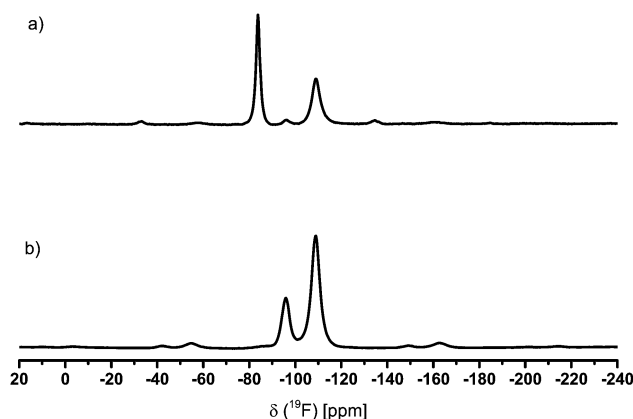

Fig. 5 ^{19}F MAS NMR spectra of CaF_2-xerogel prepared from $CaCl_2$ with one equivalent of $HF_{(EtOH)}$ (ν_{rot} = 20 kHz) dried at 40 °C (a) and (ν_{rot} = 19 kHz) 600 °C for 2 h (b).

relaxation time T_2 between the signal at −108 ppm and −95 ppm in the ^{19}F NMR spectra. According to Fig. 6 the influence of the relaxation time T_2 of under-stoichiometric xerogels reveals that the intensity of the signal at −108 ppm decreases and the intensity of the signal at −95 ppm increases. Another time-dependent NMR measurement was also performed with a CaF$_2$-xerogel derived from CaCl$_2$ with H$_2$O as solvent (Fig. 7). In the case of H$_2$O as solvent the ^{19}F NMR spectra exhibit another signal at −83 ppm beside the main signal and the signal at −95 ppm. This signal at −83 ppm corresponds to CaClF, which has the same NMR shift like the reference sample of CaClF. It is obvious that the ^{19}F signal at about −95 ppm does not correspond to the CaClF species but rather to an oxide fluoride species like CaF$_{2−x}$OR$_x$ (R = H, Et). An explanation of the formation of an oxide fluoride species from CaCl$_2$ in EtOH or in H$_2$O with ethanolic/aqueous HF-solution as fluorine agent could be either the preferential oxygen donation in the second coordination sphere like mentioned before or the use of only 96% CaCl$_2$ as precursor, which includes impurities like Ca(OH)$_2$ or CaClOH. These impurities are caused by the manufacturing process and subsequent dehydration of CaCl$_2 \cdot x$H$_2$O.[21] Thus, it could be possible that after dehydration of CaCl$_2 \cdot x$H$_2$O such oxygenated species are still present. If a certain amount of oxygen is incorporated in the CaF$_2$-film, the refractive index of the film will increase, and thus, the optical properties of such films decline. However, the percentage of oxygen is not only unwanted in CaF$_2$-films but also in ceramics due to the loss of laser oscillation as a result of the scattering at the grain boundaries, which occurs in the ceramics.[4] It is known that CaF$_2$ nanocrystals prepared by CaCl$_2$ in EtOH with NH$_4$F as fluorine agent can be also obtained *via* co-precipitation and hydrothermal synthesis.[22]

However, a certain amount of oxygen is present in the CaF$_2$ powder, which occurs from the evaporation of the precipitate. Apparently, the percentage of oxygen in the sample is induced by the drying process. Unfortunately, no ^{19}F MAS NMR spectra
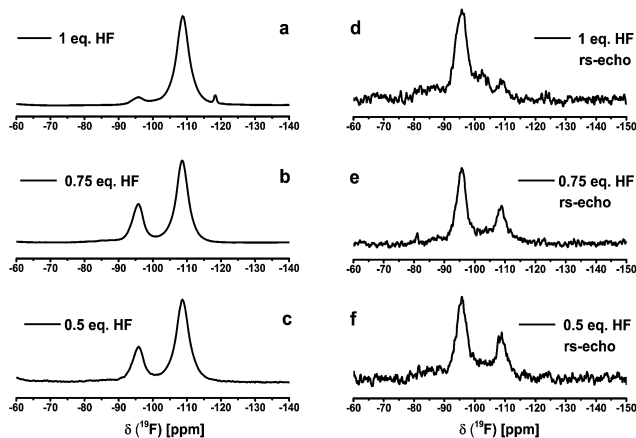

Fig. 7 ^{19}F MAS NMR spectra of CaF$_2$-xerogel derived from CaCl$_2$ in H$_2$O with two equivalents of HF$_{(EtOH)}$ (a) ν_{rot} = 25 kHz, D1 = 5 s, NS = 64 and (b) rs-echo, ν_{rot} = 20 kHz, L0 = 20, D1 = 5 s, NS = 256.

are listed in this publication, so that a comparison with the signal at −95 ppm of our shown spectra is not possible. The reflections in the X-ray pattern of the xerogels in Fig. 8 reveal CaF$_2$ and CaClF. In the diffractograms as well as in the ^{19}F NMR spectra, it is notable that the CaClF species is formed at 600 °C. Xerogels prepared from CaCl$_2$ as precursor with just one equivalent of HF show after annealing reflections of CaClF (rorisite, PDF 24-0815) and CaF$_2$ (fluorite, PDF 35-0816). In contrast, un-annealed as well as annealed xerogels obtained from stoichiometric Ca^{2+} to HF ratio show reflections of CaF$_2$ only. Obviously, the nominal fluorine stoichiometric content in the reaction of CaCl$_2$ with HF is crucial whether CaClF or CaF$_2$ is formed. The powder diffractograms show that CaF$_2$ is more crystalline in comparison to MgF$_2$. The crystallite sizes of the un-annealed CaF$_2$-xerogel derived from the Scherrer equation is

Fig. 6 ^{19}F MAS NMR spectra of xerogels with 0.5 (ν_{rot} = 19 kHz), 0.75 (ν_{rot} = 20 kHz) and 1 equivalent of HF$_{(EtOH)}$ (ν_{rot} = 20 kHz) to calcium (a–c) D1 = 5 s, NS = 64, (d) rs-echo, L0 = 20, D1 = 5 s, NS = 256, (e) rs-echo, L0 = 10, D1 = 5 s, NS = 64 and (f) rs-echo, L0 = 10, D1 = 5 s, NS = 256.
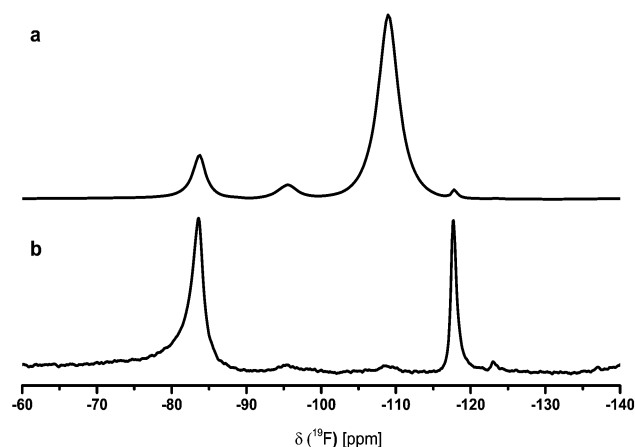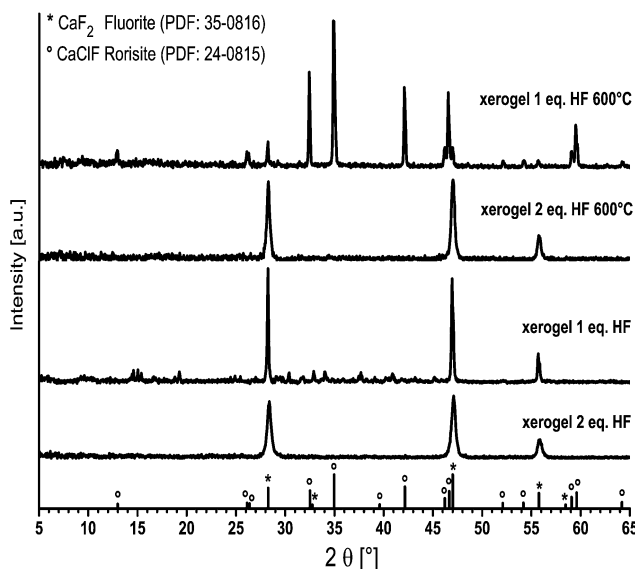

Fig. 8 X-ray diffraction patterns of un-annealed and annealed CaF$_2$-xerogels with one and two equivalents of HF$_{(EtOH)}$.

about 17 nm. In contrast, the crystallite sizes of a MgF_2-xerogel annealed at 300 °C is only about 11 nm.[17] Moreover, the chloride concentration of the xerogels, which is given in Table 1, reveals that chloride is still present. It is apparent that un-annealed as well as annealed xerogels with a stoichiometric Ca^{2+} to HF ratio still have a small chloride percentage. It shows that the fluorination of $CaCl_2$ is not complete. In case of one equivalent of HF the discrepancy of the experimentally found percentage of chloride in un-annealed and annealed xerogels is more pronounced. A plausible explanation for this effect is that the un-annealed samples contain a certain amount of water, which is caused by the hygroscopic nature of CaClF.[23] It is evident that the deviation from the experimental to the theoretical chloride percentage results from the moisture content of the environment. CaF_2-sols were used for the deposition of CaF_2-films on borosilicate glass with subsequent thermal treatment at 500 °C for 15 min. Films prepared from sols with stoichiometric fluorine content $(F^-/Ca^{2+} = 2)$ were characterised regarding their optical and mechanical properties. The optical data varied depending on the CaF_2-sol synthesis and post-treatment of the coated layer. *E.g.*, the refractive index, determined by spectroscopic ellipsometry, of a 165.50 nm thick CaF_2-film on a silicon-wafer and a post-calcination at 500 °C for 15 minutes was 1.37 at 500 nm. For CaF_2-coatings on glass the reflection and absorption of the deposited CaF_2-film were determined by UV-Vis-spectroscopy. As can be seen in Fig. 9, the reflectance at 600 nm reached almost nearly 0% and the absorbance of the layer between 400 and 900 nm is about 0% as well. Transmittance measurements of the CaF_2 film and the glass substrate were not performed for this glass sample. However, AR-layers on float glass samples from different batches showed transmission values at 600 nm repeatedly between 98.4 to 98.7%. Hence, we assume similar transmissions for this sample. Hence, the layer absorbance of CaF_2 which is given in Fig. 9 holds for the transmittance of the CaF_2 film on glass. It is the difference between the absorbance of the glass substrate and the absorbance of the glass substrate with CaF_2 film. To illustrate the morphology of the film, the cross-section image of the CaF_2-film derived from high resolution scanning electron microscopy (HR-SEM) is shown in Fig. 10. The measured thickness of the film is approximately 170 nm, and thus, corresponds very well to that determined by ellipsometry. This is in good agreement with the conditions of antireflective coatings. The diameter of the particles is between 10 and 30 nm. This corresponds well with the crystallite sizes of the xerogel determined by XRD. Furthermore, the film is very porous due to the pores, which completely proceed through the whole film. Apparently, if
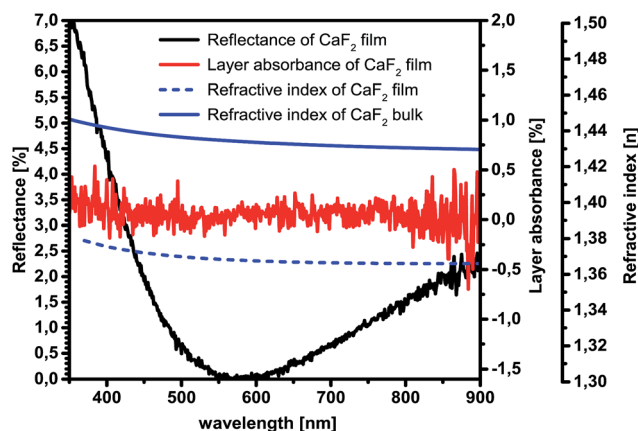

Fig. 9 Reflectance and absorption spectra of the CaF_2-film annealed at 500 °C by UV-Vis-spectroscopy and refractive index of CaF_2 film and CaF_2 bulk[24] according to the wavelength.

chloride is still present in the film, a certain amount of CaClF might be formed. Hence, the sintering process of a CaClF-containing CaF_2-film might be rendered, which is reflected by the high porosity as well mechanical abrasion (Fig. 11). Another fact causing creation of porosity could be also the release of the organic solvent together with HCl formed by the reaction of HF with $CaCl_2$. Thus, these pores filled with air $(n_0 \approx 1.0)$ are the reason for the low refractive index of the CaF_2-film. Similar porous coating films are well known for SiO_2-films on glass.[25,26] Since CaF_2 exhibits a lower refractive index than SiO_2, it was expected that CaF_2-AR-layers with lower porosity but equally good refractive indices possess higher mechanical stability. Therefore, mechanical abrasion of the films was tested too. For that purpose, the CaF_2-films annealed at 500 °C were subjected to the Crockmeter test. Fig. 11 is showing the CaF_2-film before and after abrasion with felt and steel wool. After 100 cycles with felt and 25 cycles with steel wool the film has only a slight scratch track. Under these conditions, the films are almost
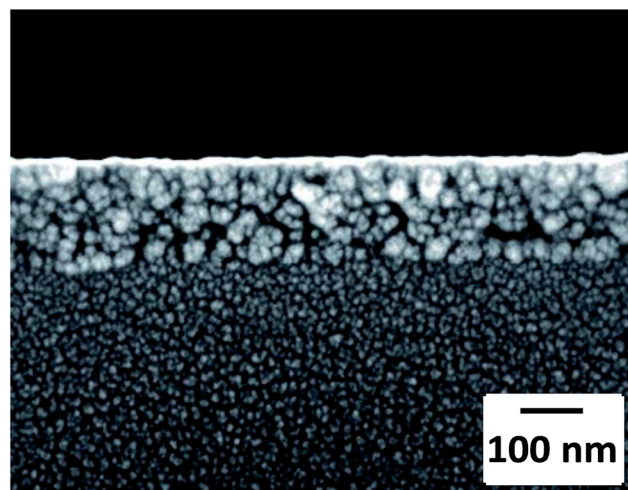
Table 1 Chloride percentage of the xerogels by elemental analysis

Xerogel	Theoretical Cl [%]	Experimental Cl [%]
1 eq. HF after 40 °C	37.50	23.42
1 eq. HF after 600 °C	37.50	34.43
2 eq. HF after 40 °C	0.0	4.16
2 eq. HF after 600 °C	0.0	2.21

Fig. 10 Cross-section image of the CaF_2-film annealed at 500 °C by HR-SEM.

This journal is © The Royal Society of Chemistry 2015
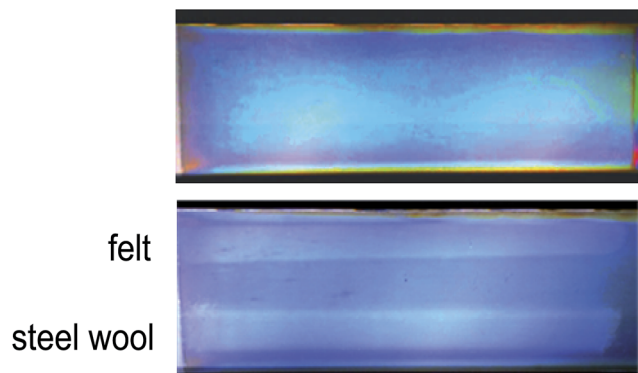
J. Mater. Chem. C, 2015, **3**, 1716–1723 | **1721**

Fig. 11 Photographs of the CaF_2-film on borosilicate glass substrate (20×4 cm^2) before and after abrasion with 100 cycles of felt and 25 cycles of steel wool by Crockmeter test. The sample has been treated at 500 °C for 15 min prior the analysis.

robust against abrasion. Just the very surface near region seems to show some little damages without losing the optical performance. There is no visual difference in the abrasion with felt or steel wool. In conclusion, the mechanical stability of CaF_2-films is better than that of other CaF_2-films, which were derived from calcium acetate as mentioned above. All in all, the CaF_2-films show not only excellent optical performance, but show at the same time also good mechanical stability.

Conclusions

The synthesis of CaF_2-sols containing nanoscopic particles was successfully performed by reaction of $CaCl_2$ as inexpensive precursor with anhydrous HF in ethanol. Addition of up to 5 mol% TMOS or TEOS after fluorination always causes a rapid formation of a transparent sol with small particle diameter in the range of 10 to 20 nm. This coating solution is stable for several weeks. No sedimentation was observed. TMOS not only causes a fast clearing up of the sol but also stabilizes the CaF_2-particles in the sol. Apparently, addition of TMOS leads to a de-agglomeration of the particles probably due to the reaction with the traces of un-reacted HF in the reaction system. We speculate that the electrostatic repulsion of the particles is changed due to the formation of $Si(OR)_{4-x}F_x$-species – even the formation of SiF_4 – as intermediate product cannot be ruled out. Since these are strong Lewis acids, the formation of a $CaSiF_6$ species might be favoured. Further investigations are necessary to study the real rule of TMOS in the CaF_2 system. We also evidenced the formation of CaClF at 600 °C beside the formation of an oxide fluoride species during the fluorination. Interestingly, the formation of CaClF is also favoured by using H_2O as solvent with two equivalents of aqueous HF-solution and subsequent drying at room temperature. The observation for the oxide fluoride species was not only recorded for $CaCl_2$ as precursor but also for other calcium precursors like calcium bromide or calcium oxide. The percentage of oxygen in the samples could be explained by dehydration of $CaCl_2 \cdot xH_2O$. It is also known that CaF_2 nanocrystals derived from $CaCl_2$ in EtOH with NH_4F, which are prepared by co-precipitation and solvothermal

technique, possess impurities of oxygen too. That could be a problem for laser applications because it leads to optical scattering losses, and hence, prohibit laser oscillation. Hence, it is difficult to completely exclude oxygen in CaF_2 nanocrystals by sol–gel as well as other synthesis techniques. The CaF_2-films exhibit excellent antireflective properties. The mechanical resistance of such films compared to CaF_2-films, which were derived from calcium acetate, is significantly better. Only corresponding MgF_2-films show marginal better mechanical resistance. It is worth noting that a further improvement of the mechanical properties of these antireflective layers is essential for applications, where a mechanical resistance is indispensable. However, due to the lower solubility as compared to MgF_2, CaF_2 is an interesting alternative candidate for the manufacture of antireflective coatings.

Acknowledgements

Notes and references

1 I. H. Malitson, *Appl. Opt.*, 1963, **2**, 1103–1107.
2 P. A. Popov, K. V. Dukel'skii, I. A. Mironov, A. N. Smirnov, P. L. Smolyanskii, P. P. Fedorov, V. V. Osiko and T. T. Basiev, *Dokl. Phys.*, 2007, **52**, 7–9.
3 I. Nicoara, M. Stef and A. Pruna, *J. Cryst. Growth*, 2008, **310**, 1470–1475.
4 A. Ikesue and Y. L. Aung, *Nat. Photonics*, 2008, **2**, 721–727.
5 M. J. Dodge, *Appl. Opt.*, 1984, **23**, 1980–1985.
6 H. K. Pulker, *Coating on glass*, Elsevier Amsterdam, 1999.
7 C. Barta, F. Fendrych, K. Recker, A. Triska and F. Wallrafen, *Cryst. Res. Technol.*, 1990, **25**, 1287–1298.
8 M. Tada, S. Fujihara and T. Kimura, *J. Mater. Res.*, 1999, **14**, 1610–1616.
9 S. Fujihara, Y. Kadota and T. Kimura, *J. Sol-Gel Sci. Technol.*, 2002, **24**, 147–154.
10 E. Kemnitz, U. Gross, S. Rudiger and C. S. Shekar, *Angew. Chem., Int. Ed.*, 2003, **42**, 4251–4254.
11 R. Sokoll, H. J. Tiller and T. Hoyer, *J. Electrochem. Soc.*, 1991, **138**, 2150–2153.
12 F. Sayilkan, M. Asilturk, H. Sayilkan, Y. Onal, M. Akarsu and E. Arpac, *Turk. J. Chem.*, 2005, **29**, 697–706.
13 B. E. Yoldas, *Am. Ceram. Soc. Bull.*, 1975, **54**, 289–290.
14 Y. L. Diao, W. P. Walawender, C. M. Sorensen, K. J. Klabunde and T. Ricke, *Chem. Mater.*, 2002, **14**, 362–368.
15 N. Y. Turova, E. P. Turevskaya, V. G. Kessler, A. I. Yanovsky and Y. T. Struchkov, *J. Chem. Soc., Chem. Commun.*, 1993, 21–23.

1722 | *J. Mater. Chem. C*, 2015, **3**, 1716–1723

This journal is © The Royal Society of Chemistry 2015

16 A. Rehmer, in *Department of chemistry*, Humboldt-Universität zu Berlin, 2012, p. 74.

17 J. Noack, K. Scheurell, E. Kemnitz, P. Garcia-Juan, H. Rau, M. Lacroix, J. Eicher, B. Lintner, T. Sontheimer, T. Hofmann, J. Hegmann, R. Jahn and P. Lobmann, *J. Mater. Chem.*, 2012, **22**, 18535–18541.

18 G. Scholz, C. Stosiek, J. Noack and E. Kemnitz, *J. Fluorine Chem.*, 2011, **132**, 1079–1085.

19 M. Karg, G. Scholz, R. Konig and E. Kemnitz, *Dalton Trans.*, 2012, **41**, 2360–2366.

20 D. A. Wenz, I. Johnson and R. D. Wolson, *J. Chem. Eng. Data*, 1969, **14**, 250–252.

21 K. M. Allal, J. C. Doliginier and G. Martin, *Oil Gas Sci. Technol.*, 1997, **52**, 361–368.

22 C. Pandurangappa, B. N. Lakshminarasappa and B. M. Nagabhushana, *J. Alloys Compd.*, 2010, **489**, 592–595.

23 H. P. Beck, *J. Solid State Chem.*, 1976, **17**, 275–282.

24 Schott Optical Glass Catalogue on August 2010.

25 Y. Liu, W. Ren, L. Y. Zhang and X. Yao, *Thin Solid Films*, 1999, **353**, 124–128.

26 N. K. Park, Y. S. Kim, M. J. Kim, T. J. Lee, S. H. Lee and S. H. Lee, *J. Nanosci. Nanotechnol.*, 2013, **13**, 7493–7497.

This journal is © The Royal Society of Chemistry 2015

J. Mater. Chem. C, 2015, **3**, 1716–1723 | **1723**